

Ship identification in sequential ISAR imagery

Atsuto Maki*, Kazuhiro Fukui

Multimedia Laboratory, Corporate Research and Development Center, TOSHIBA Corporation, 1, Komukai Toshiba-cho, Saiwai-ku, Kawasaki 212-8582 Japan

Received: 22 September 2002 / Accepted: 22 March 2004

Published online: 27 May 2004 – © Springer-Verlag 2004

Abstract. We have developed an online system that automatically identifies ships observed in a rapidly updating sequence of range-Doppler images produced by inverse synthetic aperture radar (ISAR). In the system, in order to cope with the invariable noise due to the physics of imaging, we propose to employ a multiframe image processing algorithm that stably extracts profiling as a basic feature reflecting all characteristics of a target. For ship identification, representing the extracted profiles as high-dimensional vectors, we adapt the vector analysis using the recently proposed constrained mutual subspace method (CMSM). The system currently works on an ordinary PC at 5 frames/s and achieves feasible performance of identification. The system is verified using simulated data.

Keywords: ISAR – Image sequence – Profile extraction – Constrained mutual subspace method

1 Introduction

In this paper we deal with automatic identification of ships in images produced by inverse synthetic aperture radar (ISAR). The ISAR technique is a well-established method that reconstructs a rapidly updating sequence of range-Doppler image frames of the target [3, 1].¹ Due to the physics of ISAR imaging, however, images are invariably noisy, and not all frames contain equally useful information as the imaging principle is primarily based on the target's angular motions [2]. Some previous works have thus discussed employment of multiple images as well as selection of appropriate image frames and shown the advantage for target identification [14, 10]. Those include matching of corner reflections and cumulative feature extractions to gain stability over the time variability of ISAR imagery, and different identification operations based on the maximum likelihood principle or Bayesian belief networks

have been utilized. However, the evaluation of each feature such as location of superstructure breaks or the number of major uprights requires heuristics, and one of the remaining issues is to evaluate the employed features in a more generalized framework.

The research we introduce is related to the previous approaches in that it is also based on multiframe processing, but it differs significantly in terms of both feature extraction and identification operation. The fundamental idea is to first extract as stable a characteristic as possible for identification throughout sequential frames of the range-Doppler images and represent it as a feature vector in a feature space of certain fixed dimensions so that images of a target due to different aspect angles can be treated in a unified fashion. Since the extracted characteristic, namely, the feature vector, inevitably involves variations, we design the identification process by way of subspace analysis, which is known to perform well despite variations of patterns. The thrust is thus twofold as following.

In our feature extraction we focus on profiling, a presentation of ship height structure, since it is a basic feature of the target containing all characteristics. The key technique that makes extraction of profiling possible is in a simple but effective algorithm [9]; we first detect the target range and therewith the central axis of the target so as to rectify each image and then generate a binary image with a certain threshold that we accumulate by a logical “or” operation throughout the frames for some duration. By this procedure the profiles stand out despite the background noise. More importantly, we represent the resulting profiles as high-dimensional vectors that efficiently describe the target features in terms of subspaces so that we can suitably apply the subspace method to the problem of identification. In our real-time application [8] we design the algorithm in a framework with a closed loop, as depicted in Fig. 1.

In the identification process our basic proposition is to carry out a subspace analysis [13, 11] and in particular to adapt some extensions to deal with the diversity in the appearance of targets. In the subspace method, given a set of profile patterns labeled with the ship's identity (the learning set) and an unlabeled set of profile patterns (the test set), we identify the name of each ship in the test images basically by computing

* Currently with the Graduate School of Informatics, Kyoto University

Correspondence to: A. Maki (e-mail: maki@i.kyoto-u.ac.jp)

¹ By ISAR image we mean the magnitude in the two-dimensional representation.

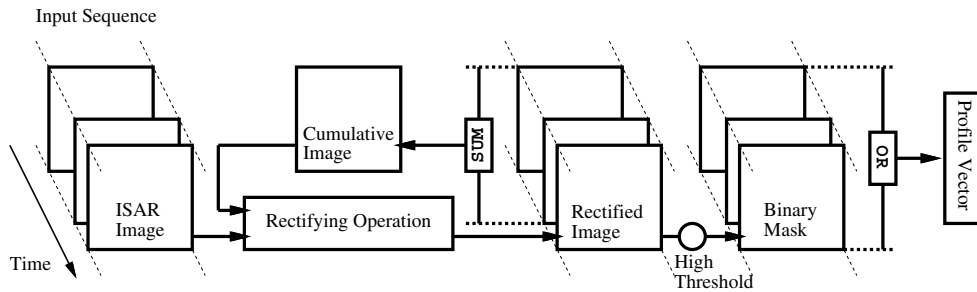


Fig. 1. Ship profiling extraction process. See also Fig. 4 for the details of the rectangular block “rectifying operation”

the similarity to the learning set. Since a large number of patterns are usually contained in the learning set, we generate a reduced number of eigenvectors by principal component analysis (PCA) and register them as dictionary patterns. Although this approach is well known within the pattern classification paradigm,² we propose to apply a further developed approach, the *constrained mutual subspace method* (CMSM);³ we compute the similarity *between subspaces* in a subspace called *constrained subspace*.

In the remainder of this paper, we first describe our technique of profile extraction in Sect. 2. Introducing CMSM as an extension of the subspace method in Sect. 3, we demonstrate the performance of the entire scheme through simulations in Sect. 4. The paper is summarized in Sect. 5.

2 Profile extraction

Range-Doppler ISAR imaging is based on target angular motions, and the Doppler frequency for a point on a rotating object is proportional to the distance from the center of rotation, measured perpendicular to the radar line-of-sight. The ISAR presentation of ship height structure thereby arising from roll and pitch is known as profiling. Since only little information is contained in one shot of a typical frame, we propose to practically extract profiling by image accumulation along the temporal axis accompanied by geometric rectification.

2.1 Geometric image rectification

In general, the appearance of a ship in ISAR imagery not only changes due to the motion of the ship but varies depending on the aspect angles. Ship identification in real ISAR data may be extremely complicated even for a human operator when the appearance is confusing, for instance, by involving the influence of yaw motion. In many situations, however, ISAR imagery of a ship tends to be a long shape oriented along the range dimension in a dark and noisy background with some clutter arising from sea waves, and in this paper we typically deal with such situations with a view to automating the task of human operators. See Fig. 2 for an example of a simulated

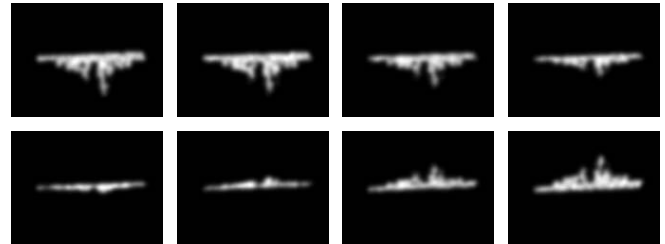


Fig. 2. ISAR simulated image sequence of ship Akz in roll motion

ISAR image sequence of a ship in roll motion. To geometrically rectify the target we need to detect the centerline. Rather than the least-square fit of target features, we try detecting the coordinates of the bow and the stern, explicitly referring to the target boundaries (at both ends of the target region in the range direction) so that the centerline can be determined as the line connecting the point of the bow through the point of the stern. See Fig. 3 for the schematic.

Although the task of detecting target boundaries is non-trivial as it is almost always obscure due to the uncertainty associated with sensor/target interaction [6], we carry it out in a cumulative image by using the presumed characteristics of the long shape of the ship target. That is, denoting the intensity of input ISAR image at coordinate (x, y) as $I(x, y)$, we first accumulate the recent (and already rectified) frames and then define in the resulting image, $I_a(x, y)$, a *boundary function*, $q(x)$, of the range (horizontal) coordinate, x , in terms of the brightness of the target region in contrast to the dark background:

$$q(x) = (h(x) - \bar{h}(x; s)) \left(\frac{C}{\bar{h}(x; s)} \right)^\alpha \tag{1}$$

$$\bar{h}(x; s) = \frac{1}{s} \sum_{k=1}^s h(x \pm k), \tag{2}$$

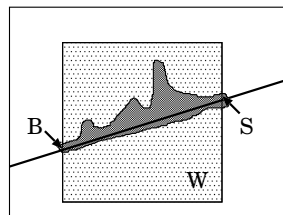


Fig. 3. Sketch of bow–stern axis. The horizontal axis corresponds to the range direction

² Similar approaches have been applied to various tasks such as character, speech, and face recognition.

³ As applied to face recognition, CMSM is shown to be effective against a diversity of illumination as well as variations of face direction or expression [4,5].

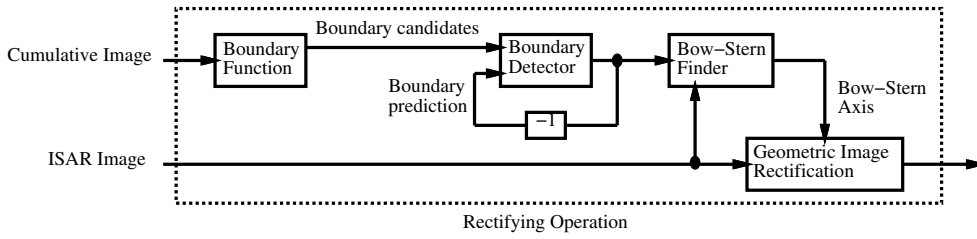


Fig. 4. Process of image rectification – details of the rectangular block “rectifying operation” in Fig. 1. The block “-1” indicates a one-frame delay in the feedback

where $h(x) = \max_y I_a(x, y)$ represents the highest intensity among the image pixels whose coordinate in the range direction is x and $\bar{h}(x; s)$ is the mean of $h(x)$ in an extent defined by s in the outer side of the image. The minus sign in Eq. 2 applies to the left half of the image and the plus sign to the right half. Note that α in Eq.1 encodes the significance of $\bar{h}(x; s)$, which inversely stresses the brightness ratio of the target edge against the background, whereas C takes a constant value for scaling.

By definition, $q(x)$ takes a relatively high value where $h(x)$ rises suddenly when searched both from the left and right end of the image and thus takes the maximum peak locally near the target boundary. Since multiple peaks may appear due to the image noise, we regard each of them as a boundary candidate and select the correct one according to the value of $q(x)$ and also to the closeness to the prediction derived from the previous frames. That is, we evaluate each candidate, x_c , by the function $e(x_c)$:

$$e(x_c) = \{1 + |x_c - x_p|\} q^{-\beta}(x_c), \quad (3)$$

where x_p is the predicted coordinate (it may simply be the position of the boundary in the previous frame) and β encodes the significance of $q(x)$. As $e(x_c)$ takes a small value for small $|x_c - x_p|$ and large $q(x_c)$, the criterion for the selection is to minimize $e(x_c)$. Denoting the selected coordinates in the left and right side as x_0 and x_1 , respectively, the target range can be roughly regarded as $x_0 \leq x \leq x_1$. Since the bow and the stern are on the boundaries and must appear as strong reflectors in the ISAR imagery, they are determined as points that have particularly high brightness in the vicinity of the peaks of $q(x)$. Figure 4 depicts the process of finding the bow–stern axis as the centerline to be used for the image rectification.

Fixing the centerline of the target by detecting the bow and the stern, we rectify each image prior to the process of accumulation in such a way that the centerline aligns with the horizontal scan line along the range direction in the center

of the image. At this stage we also judge if the target shape appears upside-down in the image according to the phase of the target motion. We make this judgment by computing the *phase ratio*, R , between the averages of the intensity on both sides of the centerline where the intensity is weighted by the distance from the centerline. That is,

$$R = I_u / I_l \quad (4)$$

$$I_u = \frac{1}{n_u} \sum_{upper} (y - c(x)) I(x, y) \quad (5)$$

$$I_l = \frac{1}{n_l} \sum_{lower} (c(x) - y) I(x, y), \quad (6)$$

where $c(x)$ indicates the vertical coordinate on the centerline and n_u and n_l are the numbers of pixels on the upper and lower side of the centerline in the rectangular region (shown as W in Fig. 3), respectively. Since the side containing the superstructure should make a higher contribution to the averaged intensity, I_u and I_l , if $R < 1$ it is judged to be upside-down and we reinvert the image along the vertical direction prior to the image accumulation. Meanwhile, if the distinction of the phase ratio turns out to be subtle ($R \simeq 1$), we do not consider the frame for further processing as it is expected to contain only little information about the structure.

Figure 5 illustrates the process of geometric rectification using an example input image of ship *Akz*. For the input image shown in Fig. 5a, the computed boundary function, $q(x)$ (computed with $s = 10$ (pixels), $C = 50$, and $\alpha = 2$ in Eq. 1), and the extracted centerline are superimposed in Fig. 5b. The range between the two high peaks of $q(x)$ at both ends is indicated by increasing the gray scale in the off-target range. Figure 5c shows the rectified image. In this example the inversion of the image with respect to the centerline occurs as the superstructure is judged to be in the lower part according to the phase ratio ($R = 0.67 < 1$). Other frames in the input sequence

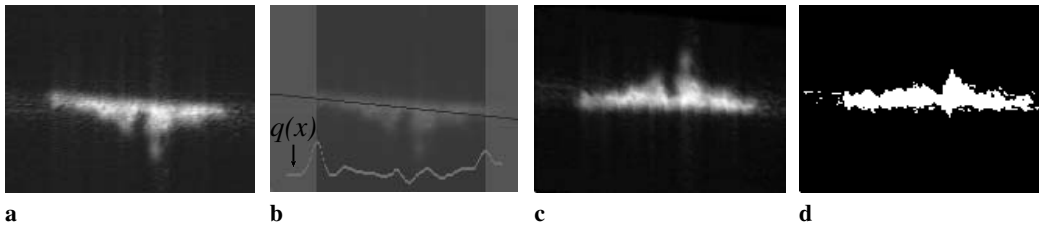


Fig. 5. **a** Sample input image frame of ship *Akz* (160×120). The target shape appears upside-down. **b** $q(x)$, the boundary function (white line), and extracted bow–stern axis (black line) are superimposed. For visualization the gray scale outside the target range is increased. **c** Rectified image according to the bow–stern axis. When it is judged to be upside-down at this stage, we reinvert the image along the vertical direction as in this example. **d** Binary image by thresholding. Note that an incomplete example is shown deliberately

are rectified analogously. It should be noted that thresholding one shot usually generates just such an incomplete binary image. Figure 5d shows an incomplete silhouette that lacks some part of the superstructure, whereas some noise from sea clutter is still present. Thus, accumulation throughout some frames takes place to generate a mask and to extract the target profile thereafter.

2.2 Image accumulation

In the second stage, we generate the profile of a target by way of accumulating the rectified images. Although multiframe processing enables us to extract different features that are likely to be present in successive image frames, simple accumulation would only emphasize regularly appearing features. In order to also preserve relatively weak but important features, with a certain threshold, I_{th} , we generate a binary image, $B_f(x, y)$, out of each geometrically rectified image, $I_n(x, y)$, throughout F frames for some duration and form a mask, $B(x, y)$, by a logical “or” of the masks. That is,

$$B_f(x, y) = \begin{cases} 1, & \text{for } I_n(x, y) > I_{th} \\ 0, & \text{for } I_n(x, y) \leq I_{th} \end{cases} \quad (7)$$

$$B(x, y) = \bigcup_{f=1}^F B_f(x, y). \quad (8)$$

Accumulation for one cycle of target motion is usually sufficient to reflect available information while avoiding the influence of the target drift. Smoothing the resulting mask, $B(x, y)$, by dilation to fill incidental holes in the mask, we obtain a simple l -dimensional representation of the profile vector as

$$p(x) = \min_y \{y \mid B(x, y) = 1, B(x, y + 1) = 0\}. \quad (9)$$

Note that we gain the computational practicality in this simplification by sacrificing some of the details in the two-dimensional mask. For the following process of identification based on the subspace method, we define $p(x)$ in certain dimensions, l , using the information in the target range, where we normalize the length so that $\|p(x)\| = 1$.

Figure 6 exemplifies the target profile vectors, $p(x)$, generated by the process of accumulation. The profile dimension, l , is aligned to be 100 (pixels). Each of these examples is the result of the logical “or” operation through a fixed number of image frames. It is observed that the profiles are extracted quite stably, though they vary slightly in details.



Fig. 6. Samples of extracted profile vectors of ship *Akz*. The dimension is aligned to be 100 (pixels), whereas the length is normalized so that $\|p(x)\| = 1$

3 Identification by subspace method

Figure 7 visualizes the eigenvectors, i.e., the principal components of the extracted profiles as exemplified in Fig. 6. Importantly, those eigenvectors span the subspace to which the

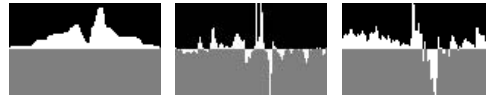


Fig. 7. Eigenvectors computed for the profile of ship *Akz*. Three eigenvectors corresponding to the three greatest eigenvalues are shown. For visualization the background of the negative components is gray colored

profiles of ship *Akz* belong in the l -dimensional space. The eigenvector corresponding to the greatest eigenvalue roughly characterizes the profile, whereas the remaining eigenvectors detail it. The eigenvectors of higher orders, however, are often contaminated by noise factors. Thus, although they describe the details of the profile, eigenvectors corresponding to a few of the major eigenvalues are employed as the bases to represent the profile of each ship.

The subspace method [11] has been widely applied to various pattern recognition tasks. It is for calculating the similarity of the angle between a vector and a subspace, i.e., the minimum angle between the test vector and the vectors that belong to the learning set. While it gives fairly good results in most tasks, it has limited recognition ability in rather complicated tasks. The *mutual subspace method* (MSM) is an extension of the subspace method where not only reference patterns (the learning set) but also input patterns (the test set) are represented with subspaces. See Fig. 8 for the concept of MSM where the two subspaces are denoted by \mathcal{P} and \mathcal{Q} . The similarity is defined by the minimum angle between the subspaces and computed as the maximum eigenvalue of a matrix. Since varieties of patterns are compared to compute the angle, MSM is suitable for recognizing multiappearance objects and achieves a high recognition rate compared with the conventional subspace method.

Although MSM is able to deal with a variety of appearances, its classification ability still appears insufficient for our task of ship identification. This is because the profiling of the ISAR presentation of ship height structure is based on the motion of the target and thereby the diversity involved in the extracted profile vectors is dependent on the type of physical target motions such as roll or pitch. Thus, the *difference vector*, $d(|u| = |v| \neq 0)$, of the two vectors, u and v , compos-

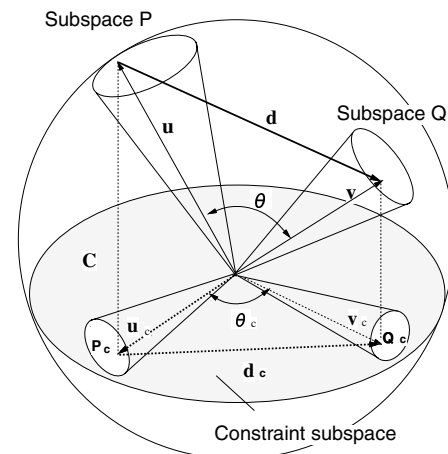


Fig. 8. Concept of MSM and CSM

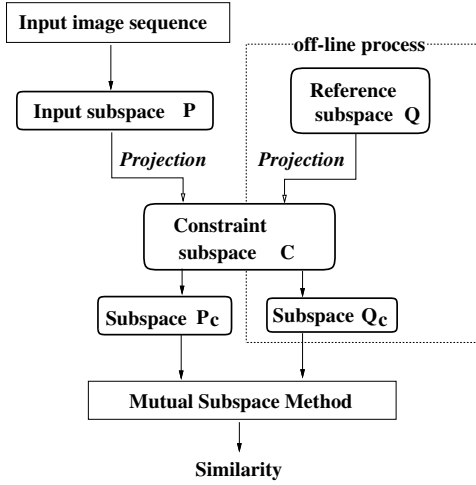


Fig. 9. Schematic of recognition process with CMSM

ing the minimum angle, θ , as sketched in Fig. 8 will include some components derived from such diversity, and the angle between the subspaces will accordingly deviate from what should be observed solely between targets. In order to attenuate the influence of such diversity, we consider employing the *constrained mutual subspace method* (CMSM) [4,5]. The essence of CMSM is to carry out MSM in a *constraint subspace* where no contribution due to the diversity of appearance is contained. See Fig. 9 for the schematic of the recognition process with CMSM. Then the issue is to effectively design a *constraint subspace* such that the robust nature of CMSM is brought out in favor of the task of ship identification. We now proceed to the formulation of MSM and CMSM.

3.1 The mutual subspace method (MSM)

As already stated, MSM utilizes the angle between two subspaces for defining the similarity between two sets of vectors. Given subspaces \mathcal{P} and \mathcal{Q} , the angle between \mathcal{P} and \mathcal{Q} is defined as the minimum angle between the vectors u and v , where $u \in \mathcal{P}$ and $v \in \mathcal{Q}$. The angle, θ , is defined as

$$\cos^2 \theta = \sup_{\substack{u \in \mathcal{P}, v \in \mathcal{Q} \\ \|u\| \neq 0, \|v\| \neq 0}} \frac{|(u, v)|^2}{\|u\|^2 \|v\|^2}. \quad (10)$$

Let M -dimensional input subspaces be \mathcal{P} , N -dimensional dictionary subspaces be \mathcal{Q} , and P and Q be orthogonal projection operators onto \mathcal{P} and \mathcal{Q} . Then the angle between \mathcal{P} and \mathcal{Q} , i.e., the similarity, is calculated as the maximum eigenvalue of PQP or QPQ [7, 12]. Further, it has been proved that the eigenvalue calculation can be practically reduced to that of lower dimensions. Let $X = (x_{ij})$ be

$$x_{ij} = \sum_{m=1}^M (\psi_i, \phi_m)(\phi_m, \psi_j), \quad (11)$$

where ϕ and ψ are the bases of P and Q , respectively. Then the eigenvalues of X are equal to those of PQP and QPQ [7], and the similarity is given as their maximum value.

3.2 The constrained mutual subspace method (CMSM)

In CMSM for ship identification it is necessary to develop a constraint such that the contribution due to the diversity in the type of ship motion is excluded from the *difference vector*, d , and we realize it by projecting d onto a *constrained subspace*, \mathcal{C} , that has no vector components arising from the diversity. As depicted in Fig. 8, the angle, θ_c , corresponding to the projected vector, d_c , approximates the angle that would be obtained by eliminating the contribution due to the diversity from θ . θ_c can also be interpreted as the angle between u_c and v_c , which are the projections of u and v on \mathcal{C} , respectively. Analogously to the angle defined in MSM, we thus formulate the similarity as the minimum angle between u_c and v_c and compute it by

$$\cos^2 \theta_c = \sup_{\substack{u \in \mathcal{P}, v \in \mathcal{Q} \\ \|Cu\| \neq 0, \|Cv\| \neq 0}} \frac{|(Cu, Cv)|^2}{\|Cu\|^2 \|Cv\|^2}, \quad (12)$$

where C denotes a matrix that projects arbitrary vectors onto \mathcal{C} .

In practice, we first compute the difference vectors for all the combinations between different targets in the learning set while only using profile vectors produced by an identical type of motion, and then define the constrained subspace, \mathcal{C} , by bases consisting of those difference vectors.

4 Experiments

We illustrate the performance of ship identification by an experiment designed with 16 image sequences of 12 different ships simulated to be in roll or pitch motions as listed in Table 1.⁴ Some examples of the simulation data are in Figs. 10 and 11. In each case the ships were simulated to proceed in the direction of 30° from the viewing angle.

Table 1. Ship database

Category	Name of ship
Learning set (Roll)	Akz, Ckg, Mng, Grc Isz, Hrn, Suy, Mur
Test set I (Pitch)	Akz, Ckg, Mng, Grc
Test set II (Roll)	Ymg, Srn, Kng, Ybr

Using eight of these image sequences, all due to roll motion, we have generated a dictionary while extracting a number of profile vectors as a learning set for each ship. Regarding the test data, we first examined four independent sequences of those ships, all synthesized due to pitch motion (we call them test set I). We have applied CMSM by defining the constrained subspace, \mathcal{C} , with the dictionary and projecting the test set as well as the learning set on \mathcal{C} . Note that the components due to the difference between types of motion should not be included in \mathcal{C} since the learning set for the dictionary is composed only of identical (roll) motion.

⁴ ISAR simulations were carried out using RIG, Radar Imagery Generator, a product of Technology Service Corp.

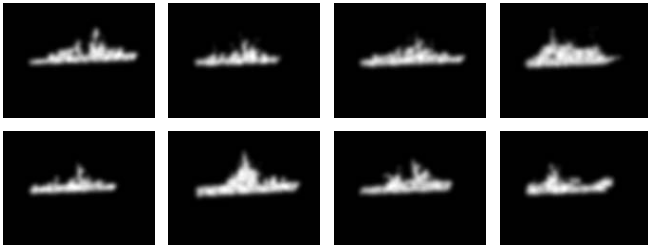


Fig. 10. Images of Learning set (by roll) – *Akz*, *Ckg*, *Mng*, *Grc*, *Isz*, *Hrn*, *Suy*, and *Mur*



Fig. 11. *Top:* Images of test set I (by pitch) – *Akz*, *Ckg*, *Mng*, and *Grc*. *Bottom:* Images of test set II (by roll) – *Ymg*, *Srn*, *Kng*, and *Ybr*

The results of the first examination are shown in the upper portion of Fig. 12. The highest similarity in each case is scored ideally (above 0.98) when compared with the correct target out of the eight candidates, whereas the scores of similarity to the other candidates are suppressed. It may then be useful to also set a threshold, T , to avoid false acceptance, for example $T = 0.6$ (see the dotted line in the graph). In a few cases the evaluations of the similarity turn out to be above the threshold while not being identical (e.g., *Ckg* vs. *Isz*). Although it is observed to be due to the resemblance in the original ship profile, the overall performance with CMSM appears satisfactory. In fact, the separability, η , as an index

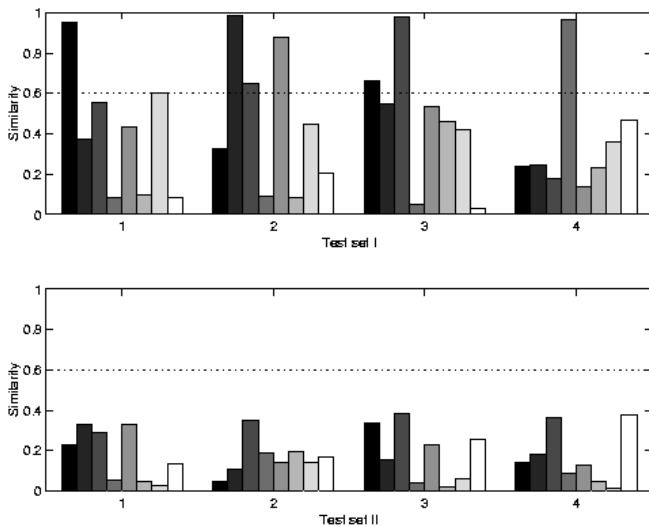


Fig. 12. Like the ship candidates, in each test the comparison is made with the 8 candidates in the dictionary (8 bars from left: *Akz*, *Ckg*, *Mng*, *Grc*, *Isz*, *Hrn*, *Suy*, and *Mur*). *Top:* Test set I (1. *Akz*, 2. *Ckg*, 3. *Mng*, and 4. *Grc*). *Bottom:* Test set II (1. *Ymg*, 2. *Srn*, 3. *Kng*, and 4. *Ybr*)

of identification ability between identities (see Appendix) has been significantly improved ($\eta = 0.506$) compared to the case of using MSM ($\eta = 0.248$). Clearer discrimination between ships with similar profilings will be an issue in future work.

We have also tested another four sequences of different ships (we call them test set II) that are not registered in the dictionary. The results are shown in the lower portion of Fig. 12. The similarity score is favorably low in each case (far smaller than the threshold), indicating the rejection performance of the method whereby the ships are not misidentified as being any of the candidates in the dictionary.

In our online implementation, the extraction of a 100-dimensional profile vector in images with 160×120 pixels and the identification of target by CMSM were continuously carried out. The frame rate to work through the entire algorithm was about 5 frames/s and the correct identification rate was above 95%.

5 Conclusion

For solving the problem of automatic ship identification in ISAR imagery, we have proposed extraction of ship profiling as the basic feature of the target patterns and adaption of the subspace analysis as a scheme of pattern recognition. In order to stably extract the profiling we introduced a simple but effective algorithm to vectorize the profile – a multiframe accumulation preceded by a precise target detection and image rectification. The algorithm is straightforward and gains stability in real-time implementation with closed loop. In the identification of the extracted profiling, we employed the constrained mutual subspace method (CMSM), and it performed well on the profile vectors despite the diversity due to the type of physical target motions. In our preliminary experiments using simulated ISAR image databases, the overall performance of the identification turned out to be satisfactory.

Future work will focus on evaluations of the algorithm for larger databases including various classes of ships with different noise levels. As we have assumed a long shape of ship oriented along the range dimension, worth investigating is also the influence of significant differences in aspect angles. Another interesting extension may be to incorporate other cues such as ship length overall, if available, for limiting the target identification to certain candidates.

Appendix: Definition of separability

Given the scores of similarity S_i between the input and the dictionary of which n_1 cases are within class and n_2 cases between classes, the separability, η , between classes is defined as

$$\eta = \frac{\sigma_b^2}{\sigma_T^2} \quad (13)$$

$$\sigma_b^2 = n_1(\bar{S}_1 - \bar{S}_m)^2 + n_2(\bar{S}_2 - \bar{S}_m)^2 \quad (14)$$

$$\sigma_T^2 = \sum_{i=1}^{n_1+n_2} (S_i - \bar{S}_m)^2, \quad (15)$$

where \bar{S}_1 , \bar{S}_2 , and \bar{S}_m denote the average of n_1 scores of similarity within a class, that of n_2 scores of similarity between

classes, and that of all the $n_1 + n_2$ scores. The higher the separability, the higher the identification ability allowing larger ranges of possible rejection threshold choices.

Acknowledgements. The authors wish to thank O. Yamaguchi for support on the online implementation and K. Maeda and K. Onoguchi for helpful discussions. They are also grateful to M. Kiya and Y. Kawawada of TOSHIBA Social Network & Infrastructure Systems Company for comments and providing the synthetic ship image data.

References

1. Ausherman DA, Kozma A, Walker JL, Jones HM, Poggio EC (1984) Developments in radar imaging. *IEEE Trans Aerospace Electron Sys* 20(4):363–398
2. Berizzi F, Diani M (1996) ISAR imaging of rolling, pitching and yawing targets. In: *Proceedings of the CIE international conference on radar*, pp 346–349
3. Chen C-C, Andrews HC (1980) Target-motion-induced radar imaging. *IEEE Trans Aerospace Electron Sys* 16:1:2–14
4. Fukui K, Yamaguchi O, Suzuki K, and Maeda K (1999) Face recognition under variable lighting condition with constrained mutual subspace method. *Trans IEICE J82-D-II(4):613–620* (in Japanese)
5. Fukui K, Yamaguchi O (2003) Face recognition using multi-viewpoint patterns for robot vision, In: *Proceedings of the 11th international symposium on robotics research*. (in press)
6. Gorin AL (1982) Effect of data reduction on inverse synthetic aperture radar (ISAR) image quality and target shape descriptions. *Opt Eng* 21(5):858–863
7. Maeda K, Watanabe S (1985) A pattern matching method with local structure. *Trans IEICE J68-D(3):345–352* (in Japanese)
8. Maki A, Fukui K, Kawawada Y, Kiya M (2002) Automatic ship identification in ISAR imagery: an on-line system using CMSM. In: *Proceedings of the IEEE radar conference*, pp 206–211
9. Maki A, Fukui K, Onoguchi K, Maeda K (2001) ISAR image analysis by subspace method: automatic extraction and identification of ship profile. In: *Proceedings of the IAPR international conference on image analysis and processing*, pp 523–528
10. Musman S, Kerr D, Bachmann C (1996) Automatic recognition of ISAR ship images. *IEEE Trans Aerospace Electron Sys* 32(4):1392–1403
11. Oja E (1983) *Subspace method of pattern recognition*. Research Studies Press, Hertfordshire, UK
12. Stewart GW (1973) *Introduction to matrix computation*. Academic Press, New York
13. Watanabe S, Pakvasa N (1973) Subspace method of pattern recognition. In: *Proceedings of the 1st international joint conference on pattern recognition*, pp 25–32
14. Yang MCK, Lee J-S (1994) Object identification from multiple images based on point matching under a general transformation. *IEEE Trans Patt Anal Mach Intell* 16(7):751–756